Momentum distributions in stripping reactions of single-nucleon halo nuclei

H. Esbensen
Physics Division, Argonne National Laboratory, Argonne, Illinois 60439
(Received 29 November 1995)

The widths of the longitudinal momentum distributions of projectilelike fragments produced in (^{11}Be, ^{10}Be$+n$) and in (^{8}B,^{7}Be$+p$) breakup reactions are analyzed using a single-particle description. The strong absorption limit of the Serber model reproduces both data sets quite accurately. The transparent limit, on the other hand, can reproduce the width of the ^{11}Be data reasonably well but it fails dramatically for the ^{8}B data. The reason is that the absorption of the projectilelike fragment has a much larger effect on the width when the orbital angular momentum of the valence nucleon is nonzero.

PACS number(s): 25.60.Gc, 25.70.Mn

The longitudinal momentum distribution (LMD) of projectilelike fragments, observed in the two-body breakup of a halo nucleus, is often compared to, and sometimes identified with, the ground state momentum distribution of the two fragments. This identification is realistic if the basic breakup mechanism is stripping and the target nucleus is completely transparent to the observed fragment. This is one of the limits that was considered by Serber in his study of the neutron production in deuteron stripping reactions [1], and it is often referred to as the Serber model.

The LMD of ^{10}Be fragments, produced in the breakup of ^{11}Be, has recently been measured on a beryllium target at 63 MeV/nucleon [2], and it was shown that the observed width can be reproduced quite well in the transparent limit of the Serber model. It was therefore surprising that this limit failed and gave a much broader distribution than observed in the (^{8}B,^{7}Be$+p$) breakup on a carbon target at 1471 MeV/nucleon [3]. In the following it is demonstrated that this failure is due to the neglect of absorption. It is shown that absorption plays a crucial role for the width of the LMD if the valence nucleon is in a p-wave (e.g., ^{8}B), while it has only a minor effect if it is bound in an s wave (e.g., ^{11}Be).

In his original work [1], Serber also considered the more realistic opaque (or strong absorption) limit, where the absorption of the observed particle is taken into account. This approach has more recently been applied to the cluster breakup of halo nuclei [4–8]. This model is adopted in the following and it is applied to the stripping of single-nucleon halo nuclei: $a \rightarrow c + x$, where x is the valence nucleon that is absorbed by the target nucleus and c is the detected core fragment.

The basic expression for the momentum distribution of corelike fragments in stripping reactions is

$$\left(\frac{d\sigma}{d\mathbf{k}}\right)_{\rm str} = \int d^{(2)}\mathbf{b}_x (1-|S_{xt}(b_x)|^2)\frac{dP(\mathbf{k},\mathbf{b}_x)}{d\mathbf{k}}. \qquad (1)$$

The two-dimensional integration is over all impact parameters b_x of the valence nucleon x with respect to the target. The function S_{xt} is the so-called profile function (or S matrix) for the scattering of nucleon x on the target nucleus t.

The last factor in Eq. (1) is the momentum distribution of the corelike fragment for a fixed value of b_x,

$$\frac{dP(\mathbf{k},\mathbf{b}_x)}{d\mathbf{k}} = \frac{1}{(2\pi)^3(2j+1)}\sum_{m,m_s} |\langle e^{-i\mathbf{kr}}\chi_{m_s}|S_{ct}(|\mathbf{b}_x-\mathbf{r}_\perp|)|\psi^{(gs)}_{\ell jm}(\mathbf{r})\rangle|^2. \qquad (2)$$

It contains the matrix element of a similar profile function, S_{ct}, for the interaction of the core fragment c with the target nucleus t. The ground state wave function of the halo nucleus is here assumed to have the usual single-particle form,

$$\Psi^{(gs)}_{\ell jm}(\mathbf{r}) = \frac{\phi_{\ell j}(r)}{r}\sum_{m_\ell m_s}\langle \ell m_\ell \tfrac{1}{2} m_s | jm\rangle \chi_{m_s} Y_{\ell m_\ell}(\hat{r}), \quad (3)$$

and Eq. (2) includes an average sum over the m substates. The final state of the core fragment is assumed to be a simple plane wave, and Eq. (2) also includes a sum over the two spin projections, $m_s = \pm 1/2$, of the absorbed nucleon.

The profile functions can be calculated in an eikonal approximation, for example as it was done in Refs. [9,10] from the free nucleon-nucleon scattering. A simpler approximation that is often used is the black disc model [1,5,6,8],

$$S_{it}(b) = 0, \quad b \leq R_{it}, \quad S_{it}(b) = 1, \quad b > R_{it}, \qquad (4)$$

where $i = x$ or c represents the valence nucleon or the core fragment, respectively. This approximation will be used in the following. Other, more realistic, diffuse profile functions have also been used [4,7].

There is an additional contribution to the momentum distribution due to diffraction. The valence nucleon is not ab-

sorbed in this case but it is emitted into the continuum due to the nuclear interaction with the target nucleus [6–8]. This contribution is more difficult to calculate because it requires realistic wave functions for the relative motion of the emitted nucleon and the corelike fragment in the final states. It has so far only been considered in cases where the ground state has been approximated by a simple Yukawa type wave function [6–8]. The diffraction component is neglected in the following. Coulomb dissociation is also ignored, since we shall only consider light target nuclei.

Before the results of detailed calculations are presented, let us first consider the simpler, transparent limit of the Serber model. Thus, if we put the core-target profile function, S_{ct}, equal to one in Eq. (2) we just obtain the ground state momentum distribution. For a particular m substate this distribution is

$$\left(\frac{dP(\mathbf{k})}{d\mathbf{k}}\right)_m = \frac{2|R_{\ell j}(k)|^2}{\pi k^2} \sum_{m_s m_\ell} \langle \ell m_\ell 1/2 m_s | j m\rangle^2 |Y_{\ell m_\ell}(\hat{k})|^2, \quad (5)$$

where the radial integral is

$$R_{\ell j}(k) = \int_0^\infty dr k r j_\ell(kr) \phi_{\ell j}(r). \quad (6)$$

The average ground state momentum distribution that one obtains from Eq. (5) is

$$\left(\frac{dP(\mathbf{k})}{d\mathbf{k}}\right)_{\text{ave}} = \frac{2|R_{\ell j}(k)|^2}{\pi k^2} \frac{1}{2\ell+1} \sum_{m_\ell} |Y_{\ell m_\ell}(\hat{k})|^2 = \frac{|R_{\ell j}(k)|^2}{2\pi^2 k^2}. \quad (7)$$

The associated longitudinal momentum distribution, obtained by integrating Eq. (7) over all transverse momenta, is

$$\left(\frac{dP(k_L)}{dk_L}\right)_{\text{ave}} = \frac{1}{\pi} \int_{|k_L|}^\infty \frac{dk}{k} |R_{\ell j}(k)|^2. \quad (8)$$

This expression gives a reasonable estimate of the width of the measured LMD of ^{10}Be fragments emitted in the breakup of ^{11}Be [2]. However, it fails for the ^{8}B breakup; the measured width (FWHM) of the ^{7}Be LMD is 81 ± 6 MeV/c, whereas Eq. (8) predicts a width that is about twice as large [3].

In order to understand the above discrepancy it is important to realize that the transparent limit is unrealistic, i.e., the absorption of the core fragment cannot in general be neglected. This is particularly obvious when one wants to account for measured breakup cross sections but we are here mainly concerned with the width of the LMD. We shall see that the opposite limit, namely the opaque (or strong absorption) limit, is more realistic. In fact, Serber came to the same conclusion in his original work [1] on the energy distribution of neutrons produced in stripping reactions of deuterons.

The crucial point in the present context is that the valence neutron in ^{11}Be is mainly bound in an s wave [11], whereas

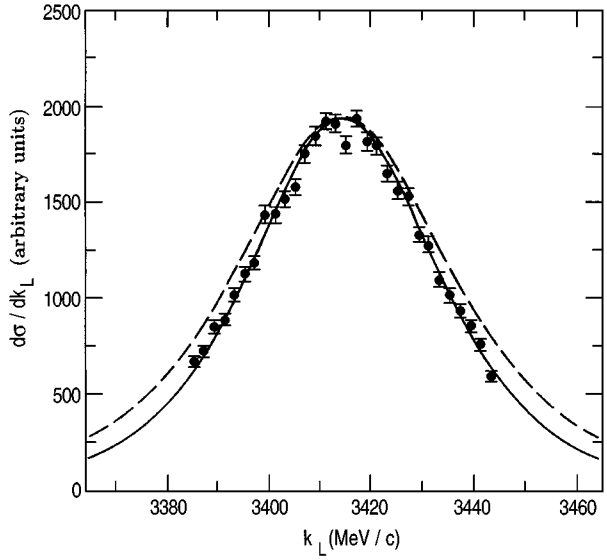

FIG. 1. Longitudinal momentum distributions of ^{10}Be fragments in the laboratory frame, from the breakup of ^{11}Be at 63 MeV/nucleon on a ^{9}Be target. The data are from Ref. [2], and the curves have been normalized to match the measured peak height. The dashed curve is the result obtained in the transparent limit and the solid curve is from the opaque (or black disc) limit of the Serber model.

the valence proton in ^{8}B is mainly bound in a $p_{3/2}$ orbit [12]. One can easily illustrate the effect of absorption in the case of ^{8}B (i.e., for a p wave) by considering the dependence on the orientation of the single-particle orbit. Here it is convenient to choose the z axis along the beam direction. Then it appears obvious that the most dominant production of ^{7}Be fragments will occur when $m_\ell = \pm 1$. The proton orbit will

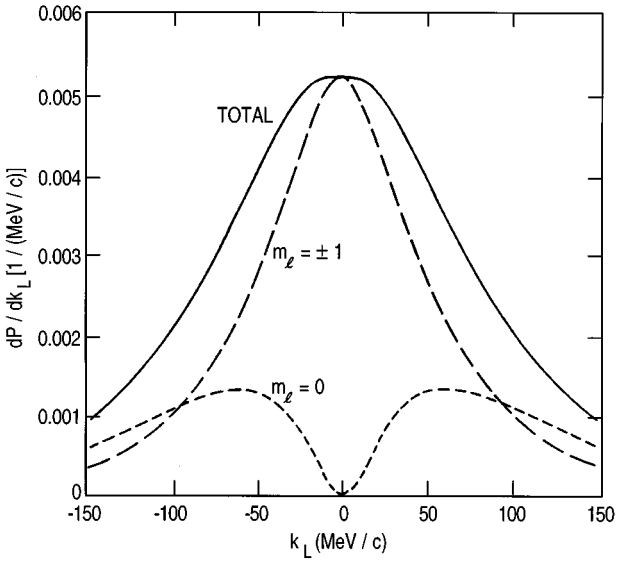

FIG. 2. The solid curve is the average longitudinal momentum distribution of the ^{7}Be core in the ground state of ^{8}B. This is the result one obtains in the transparent limit of the Serber model. The dashed curves are the two separate contributions from $m_\ell = 0$ and $m_\ell = \pm 1$ discussed in the text.

then stick out perpendicular to the projectile trajectory, and it can hit the target nucleus, while the core can stay farther away and survive the collision. When $m_\ell = 0$, the proton orbit is aligned with the ^{8}B trajectory. If the proton hits the target nucleus, then it is also quite likely that the ^{7}Be core will hit the target and get absorbed.

Based on the above geometric picture of the absorption process, one can make a crude estimate of the LMD for an initial p wave simply by neglecting the $m_\ell = 0$ contribution. This approximation leads to a large reduction in the width of the LMD. This can be seen by considering the LMD one obtains in the transparent limit from the two remaining contributions, from $m_\ell = \pm 1$. The latter distribution can easily be determined from Eq. (7),

$$\sum_{m_\ell = \pm 1} \left(\frac{dP}{dk_L} \right)_{m_\ell} = \frac{1}{\pi} \int_{|k_L|}^{\infty} \frac{dk}{k} |R_{\ell j}(k)|^2 \sin^2(\theta_k), \qquad (9)$$

where $\sin^2(\theta_k) = 1 - (k_L/k)^2$. The last factor reduces the width of the ^{7}Be LMD, as discussed below in connection with Fig. 2, from 166 to about 104 MeV/c (FWHM).

Let us now return to the more realistic estimate of LMD that is based on Eqs. (1)–(4). By integrating over all transverse momenta one obtains an expression that is local in the transverse coordinates. Moreover, by inserting the single-particle wave function (3) into Eq. (2) one can perform the sums over m and m_s and obtain,

$$\left(\frac{d\sigma}{dk_L} \right)_{\rm str} = \int d^{(2)}\mathbf{b}_x (1 - |S_{xt}(b_x)|^2) \int d^{(2)}\mathbf{r}_\perp |S_{ct}(|\mathbf{b}_x - \mathbf{r}_\perp|)|^2 \frac{1}{2\pi(2\ell+1)} \sum_{m_\ell} \left| \int dz e^{-ik_L z} \frac{1}{r} \phi_{\ell j}(r) Y_{\ell m_\ell}(\hat{r}) \right|^2 . \qquad (10)$$

This expression clearly shows how the LMD for stripping probes the ground state wave function. One feature is that it contains the geometrical aspects of absorption for p waves discussed above. Another feature is that the LMD probes mainly the tail of the single-particle wave function, at larger values of $r_\perp$, where the LMD is narrower. These features are illustrated below.

The interaction of the valence nucleon with the core is parametrized as a Woods-Saxon well, with diffuseness $a = 0.52$ fm and radius R_{xc}, and it is supplemented with the Coulomb interaction in the case of a valence proton. The well depth is adjusted to reproduce the known binding energy. The black disc model, Eq. (4), is used for simplicity to model the absorption. The associated radii are parameterized as $R_{ct} = r_{\rm abs}(A_c^{1/3} + A_t^{1/3})$ for the core, and $R_{xt} = r_{\rm abs} A_t^{1/3} + 0.8$ fm for the valence nucleon [8]. Results are shown for $r_{\rm abs} = 1.5$ fm, and the sensitivity to this parameter is discussed.

The valence neutron in ^{11}Be is mainly bound in a $2s_{1/2}$ single-particle state (i.e., an excited s wave which has one node), and we choose $R_{xc} = 2.7$ fm. The two LMD's of ^{10}Be fragments that one obtains in this case for a beryllium target are shown in Fig. 1 together with the data of Ref. [2]. The dashed curve is transparent limit, Eq. (8), and the solid curve is the opaque limit of the Serber model, Eqs. (4) and (10). The calculated LMD's have here been transformed into the laboratory frame of the experiment and they have been normalized to match the peak height. The effect of absorption is seen to be quite modest in this case. In the rest frame of the ^{11}Be, the width (FWHM) is reduced from 46.5 to 40.7 MeV/c. The latter value is consistent with the measured width [2], of 41.6 $\pm$ 2.1 MeV/c.

In this connection it is also interesting to quote the results one obtains from the simple Yukawa wave function that is commonly used in the study of halo nuclei and which has the correct asymptotic form for an s wave. The width of the LMD that one obtains for this wave function is 58.6 MeV/c in the transparent limit, and it is reduced to 40.8 MeV/c in the opaque limit. The latter result is almost identical to the value obtained above from the more realistic $2s_{1/2}$ single-particle wave function. This result clearly confirms the second feature mentioned below Eq. (10), namely that the opaque limit probes mainly the tail of the single-particle wave function.

The $p_{3/2}$ wave function of the valence proton in ^{8}B is calculated from the single-particle Hamiltonian used in Ref. [13]. The nuclear interaction used there includes a spin-orbit term but it is essentially equivalent to a pure Woods-Saxon well with a radius of 2.48 fm for a $p_{3/2}$ state. The ground state LMD obtained from Eq. (8) is illustrated by the solid curve in Fig. 2. It has a width of 166 MeV/c. This result represents the transparent limit of the Serber model.

Also shown in Fig. 2 are the two separate contributions from $m_\ell = \pm 1$, Eq. (9), and from $m_\ell = 0$. The latter distribution can be obtained from Eq. (9) simply by replacing the factor $\sin^2(\theta_k)$ by $\cos^2(\theta_k) = (k_L/k)^2$. It is seen to be quite broad and it vanishes for $k_L = 0$. The large width is due to the fact that the kinetic energy inside the core is larger in the z direction than in the two transverse directions in this particular substate. This feature of a p wave is particularly evident in a three-dimensional harmonic oscillator model. The contribution from $m_\ell = \pm 1$ represents the crude geometric estimate, Eq. (9). It has a width of 104 MeV/c.

The corresponding three LMD's one obtains in the opaque limit, Eqs. (4) and (10), are shown in Fig. 3 for a carbon target. It is seen that the $m_\ell = 0$ contribution is strongly reduced in comparison to Fig. 2, in particular in the tails at large momenta. The width of the $m_\ell = \pm 1$ distribution is also reduced, from 104 to 64 MeV/c. These reductions are both consistent with the two qualitative features discussed below Eq. (10). The solid curve in Fig. 3 shows the total LMD. It has a width of 82 MeV/c, consistent with the the measured value [3] of 81 $\pm$ 6 MeV/c. Comparing this distribution to Fig. 2 it is seen that the crude geometric estimate [Eq. (9), the dashed curve in Fig. 2 with $m_\ell = \pm 1$] gives a more realistic estimate than the transparent limit does (the

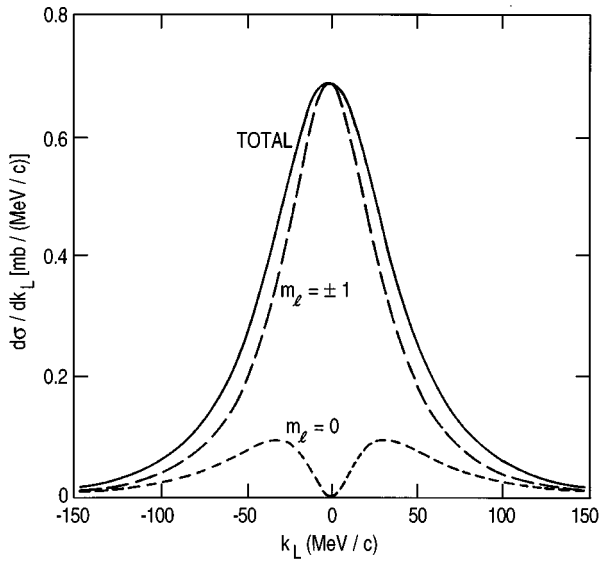

FIG. 3. Average longitudinal momentum distribution of ^{7}Be fragments (solid curve) from stripping reactions of ^{8}B on a carbon target, calculated in the opaque (or black disc) limit of the Serber model. The dashed curves are the two separated contributions from $m_\ell = 0$ and $m_\ell = \pm 1$ discussed in the text.

solid curve in Fig. 2). However, the crude geometric estimate is not sufficiently accurate at a quantitative level.

The (^{8}B,^{7}Be) stripping cross section obtained from Eqs. (4) and (10) is 68 mb whereas the measured cross section is 94 $\pm$ 4 mb [3]. There is of course some uncertainty in the choice of r_{abs}. If we reduce the value of this parameter, from 1.5 to 1.25 fm, the stripping cross section increases from 68 to 78 mb, and the width of the LDM increases from 82 to 91 MeV/c. If we instead increase the radius of the Woods-Saxon well by 0.3 fm, the stripping cross section increases from 68 to 77 mb, whereas the width of the LMD is insensitive to this variation. Thus it appears that stripping can account for a major fraction of the measured cross section.

In order to get a better understanding of the nuclear induced breakup process it would be very useful to have measurements, both of the cross section and the width of the LMD, over a wide range of beam energies. To calibrate or test the absorption as a function of beam energy, it would be important also to include the contribution from diffraction in the calculated cross section and LMD. Work in this direction is currently being pursued, using more realistic, diffuse profile functions. Preliminary results show that the diffraction component is quite sensitive to the diffuseness of the profile functions, whereas the stripping component is more stable. An alternative insight into the breakup mechanisms may be obtained from multiplicity measurements. The multiplicity of protons in the (^{8}B,^{7}Be) breakup, or of neutrons in the (^{11}Be,^{10}Be) breakup, must be related to the relative yield of diffraction events. However, it may be difficult in an actual measurement to clearly distinguish between stripping and diffraction events [14].

Apart from uncertainties in the total cross section, it appears that the width of the observed LMD of ^{7}Be fragments [3] is consistent with the opaque (or strong absorption) limit of the Serber model, whereas the transparent limit grossly overestimates the width. This conclusion is based on a single-particle description of the valence proton in ^{8}B, with a $p_{3/2}$ ground state wave function. The conclusion made in Ref. [3], namely that a mean field (or single-particle) description cannot reproduce the ^{8}B data, is clearly misleading because the analysis made there was based on the transparent limit of the Serber model.

The author is grateful to Sam Austin and John Kelley for stimulating discussions. This work was supported by the U.S. Department of Energy, Nuclear Physics Division, under Contract No. W-31-109-ENG-38.

[1] R. Serber, Phys. Rev. **72**, 1008 (1947).
[2] J. H. Kelley *et al.*, Phys. Rev. Lett. **74**, 30 (1995).
[3] W. Schwab *et al.*, Z. Phys. A **350**, 283 (1995).
[4] C. A. Bertulani and K. W. McVoy, Phys. Rev. C **46**, 2638 (1992).
[5] H. Sagawa and N. Takigawa, Phys. Rev. C **50**, 985 (1994).
[6] F. Barranco, E. Vigezzi, and R. A. Broglia, Phys. Lett. B **319**, 387 (1993).
[7] P. Banerjee and R. Shyam, Phys. Lett. B **349**, 421 (1995).
[8] F. Barranco, E. Vigezzi, and R. A. Broglia, University of Milano Report No. NTGMI-95-2, 1995.
[9] G. Bertsch, H. Esbensen, and A. Sustich, Phys. Rev. C **42**, 758 (1990).
[10] Y. Ogawa, K. Yabana, and Y. Suzuki, Nucl. Phys. A **543**, 722 (1992); **571**, 784 (1994).
[11] H. Sagawa, B. A. Brown, and H. Esbensen, Phys. Lett. B **309**, 1 (1993); Phys. Rev. C **51**, 1274 (1995).
[12] B. A. Brown, A. Csoto, and R. Sherr, Nucl. Phys. **A597**, 66 (1996).
[13] H. Esbensen and G. F. Bertsch, Phys. Lett. B **359**, 13 (1995).
[14] R. Anne *et al.*, Nucl. Phys. A **575**, 125 (1994).